Proceedings of the Fifteenth International Conference on
Computational Structures Technology
Edited by: P. Iványi, J. Kruis and B.H.V. Topping
Civil-Comp Conferences, Volume 9, Paper 7.3
Civil-Comp Press, Edinburgh, United Kingdom, 2024
ISSN: 2753-3239, doi: 10.4203/ccc.9.7.3

Objectivity and Consistency of the Cracking Response of RC Beams with Conventional Models

L. Parente[1], D. Addessi[2], B. A. Izzuddin[3] and E. Spacone[1]

[1] Department of Engineering and Geology, University of Chieti-Pescara G. D'Annunzio, Italy
[2] Department of Structural and Geotechnical Engineering, Sapienza, University of Rome, Italy
[3] Department of Civil and Environmental Engineering, Imperial College London, London, United Kingdom

Abstract

This study addresses model objectivity and consistency in the finite element analysis of reinforced concrete (RC) beams, with a particular focus on bond-slip effects. Classical beam finite element models often assume a perfect bond between concrete and steel reinforcement, leading to inaccuracies in simulating crack initiation and propagation. The behaviors of both displacement-based (DB) and force-based (FB) beam models are explored. Fracture energy-based regularization techniques are used to address mesh dependency and the limitations of the plane section assumption. The paper presents a detailed analysis of perfect-bond and bond-slip models within the DB and FB frameworks, highlighting their effectiveness in capturing the complex interactions in RC structures. Through practical applications and test cases, the performances of the above models are investigated, emphasizing the importance of upgrading existing models and their capability to predict structural behavior in presence of cracking

phenomena. Possible enhancements for these models, including higher-order shape functions and advanced numerical integration techniques are discussed. While the problem of localization in compression (crushing) has been extensively studied and solutions have been developed, this work specifically focuses on the localization that occurs at the onset of cracking.

Keywords: beam elements, fiber modeling, bond-slip, concrete damage plasticity, reinforced concrete, regularization.

1 Introduction

Beam finite elements are essential tools in the structural analysis of reinforced concrete (RC) beams. Despite numerous advancements, classical beam models still face challenges in accurately representing some critical phenomena, such as bond-slip interaction and cracking [1, 2]. This paper addresses these limitations by exploring numerical issues when using standard finite element models, with a focus on bond-slip effects. Beam finite element models have evolved significantly, with two main formulations forming the basis of their development: displacement-based (DB) and force-based (FB) approaches.

DB models approximate the displacement fields within the element, and derive the stiffness matrix from the derivatives of the displacement shape functions. These models are widely used due to their simplicity and ease of implementation. However, the assumed displacement fields become highly approximated and lead to inaccurate solutions when severe nonlinearities develop, thus requiring fine meshes to improve numerical results. There may also be numerical instability and convergence issues, especially when dealing with large deformations or complex loading conditions [3].

In contrast, FB models assume exact internal forces in classical Euler-Bernoulli and Timoshenko beam elements, ensuring force equilibrium at each computational step. An involved FE implementation procedure is however needed to implement FB models in general purpose FE codes as the element naturally derives flexibility rather than stiffness matrix. The approach allows capturing the nonlinear behavior and complex loading scenarios often using a single beam model per structural member, making it highly effective for detailed nonlinear structural analyses [4, 5, 6].

Both DB and FB models are frequently coupled with fiber section models that accurately describe the bidirectional PMM (axial force-moment-curvature) interaction. The selection of appropriate material laws is crucial for achieving accurate analyses. Enhancements in both DB and FB formulations have been developed over the years to improve their accuracy and computational efficiency. These include the use of higher-order shape functions, advanced numerical integration techniques, and refined material models that better capture the nonlinear characteristics of RC structures. Addressing mesh dependency in finite element analysis, particularly in scenarios involving material softening such as concrete cracking and crushing is critical. Regularization

techniques, such as nonlocal damage models and gradient-enhanced formulations, are crucial in ensuring that numerical results are objective and mesh-independent, especially when localized damage or fracture occurs [7, 6, 8, 9].

Advancements in beam finite element models have also included enhanced section kinematics. Traditional beam models assume the hypothesis that plane sections remain plane. Although this assumption is the most commonly used, it restricts the model's ability to simulate complex deformation patterns accurately under Euler-Bernoulli assumptions. However, this rigid plane section assumption is often inadequate for specific applications. For instance, thin-walled beams can exhibit significant warping and distortions [10]. Deep beams and those under torsional loading often experience non-planar deformations and shear lag effects [11]. Curved beams or those subjected to dynamic loading also fail to comply with the plane section hypothesis due to complex deformation modes [12]. By incorporating enhanced kinematic descriptions, and introducing warping deformation modes, these models can more accurately represent the true behavior of RC beams under various loading conditions [13, 14].

Addessi et al. [13] developed enriched beam models that incorporate warping, significantly improving the simulation of torsional and warping effects. This enhancement is crucial for accurately capturing the detailed deformation patterns in RC beams, particularly under scenarios involving cracking or discontinuities. The interaction between concrete and reinforcements in RC beams, particularly bond-slip behavior, is a critical aspect that classical beam models often fail to capture accurately. The assumption of a perfect bond between concrete and steel reinforcement can lead to significant inaccuracies in predicting the structural response, especially in terms of crack initiation and propagation [14].

To address these challenges, bond-slip can be considered in different ways within both DB and FB frameworks. Explicit bond-slip models incorporate the bond-slip relationship into the FE formulation explicitly detailing each element in a system of frames and trusses. This approach provides a direct introduction at a global level of the relative displacements between the concrete and steel reinforcement, by using a force-slip spring. Implicit models incorporate bond-slip effects in the element formulation, either through modified material models, boundary conditions, additional degrees of freedom, or enhanced interpolations. These offer a practical solution for including bond-slip effects without significantly increasing the number of elements and therefore degrees of freedom [14, 15, 16, 17, 18]

Sio et al. [14] have extensively explored both explicit and implicit bond-slip models, demonstrating their effectiveness in capturing the interactions between reinforcement and concrete. These models are pivotal for improving the accuracy of beam finite element analyses, particularly in scenarios involving significant bond-slip phenomena.

This paper is structured to address the numerical challenges in beam finite element formulations with a focus on bond-slip effects. The following sections are organized as follows:

- Beam Finite Elements with Bond-Slip: This section introduces the various models used in this study, including classical beam elements with perfect-bond as-

sumptions and those incorporating bond-slip via the explicit modeling approach.
- Results: This section presents practical applications and test cases. It explores bending tests on plain concrete and RC beams with perfect-bond and bond-slip models, examining how these models perform under different conditions and highlighting mesh-dependency issues.

The simulations are run in OpenSEES [19] and STKO [20] is used to process the results.

2 Beam elements with bond-slip

The following section outlines the beam elements used in the numerical framework for nonlinear structural analyses. These elements are based on the following assumptions:

- the study focuses on slender beams, under the Euler-Bernoulli beam theory. This assumption helps emphasize objectivity issues, considering only flexural failure in the analyses;
- all cases are analyzed within a two-dimensional framework, involving only reinforced concrete (RC) planar subsystems;
- a fiber section approach is used to model the generalized nonlinear constitutive behavior of concrete at the section level;
- steel rebars are modeled using truss elements;
- rigid links and unidirectional springs are used to model the bond-slip behavior between the concrete fiber section and the steel rebars;
- uniaxial constitutive laws describe both the concrete fibers and the steel trusses response. Finally, a bond-slip relationship is assigned to the unidirectional springs that represents the bond interface.

2.1 Beam models

This section describes the beam models used in the nonlinear structural analysis framework. It focuses on perfect-bond models and their applications with the well-known displacement based (DB) and force-based (FB) approaches. In the DB approach, displacement shape functions are assumed along the element and the beam strains are derived using from the displacement fields by the compatibility equations. Weak equilibrium is imposed to find the element stiffness matrix and nodal forces. Conversely, in the FB approach equilibrated force distributions are assumed along the element. Weak compatibility yields the element flexibility matrix and nodal basic displacements. Numerical procedures are used to implement FB elements in standard DB FE programs.

The nodal displacements in the element local reference system $\mathbf{u}_l$ and their dual forces $\mathbf{p}_l$ are defined as shown in Fig. 1a:

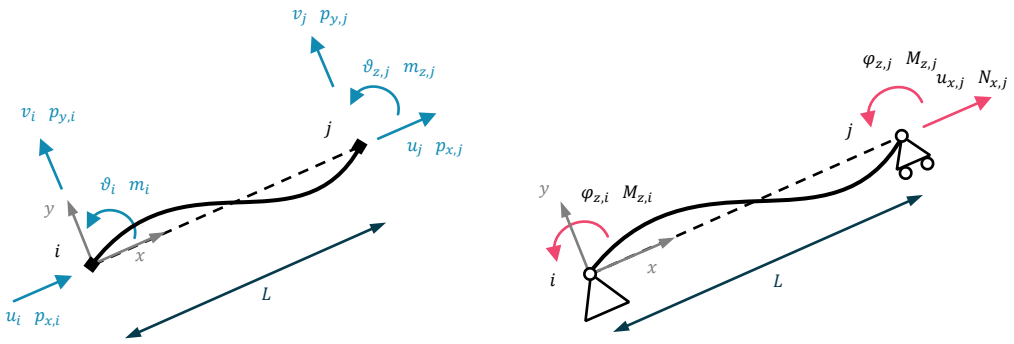

(a) (b)

Figure 1: Beam element nodal displacements and forces in the (a) local and (b) basic reference system.

$$\mathbf{u}_l = \{u_i \quad v_i \quad \vartheta_{z,i} \quad u_j \quad v_j \quad \vartheta_{z,j}\}^T, \quad \mathbf{p}_l = \{p_{x,i} \quad p_{y,i} \quad m_{z,i} \quad p_{x,j} \quad p_{y,j} \quad m_{z,j}\}^T \tag{1}$$

Two models are considered in this paper:

1. Perfect bond fiber-section models

2. Explicit bond-slip models

In the former, the steel rebars are discretized as fibers fully bonded to the concrete fibers. In the latter, the steel rebars are modeled explicitly as truss elements connected to the beam element through nonlinear nodal springs that allow relative displacements and then a bond-slip relationship. Figs. 2 and 3 show the numerical setups that introduce bond-slip between beam and truss elements.

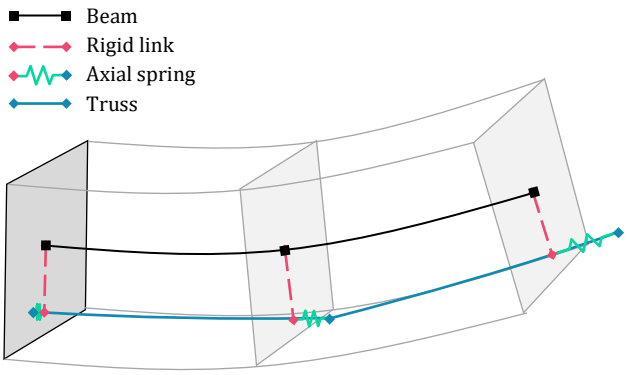

Figure 2: Explicit configuration of beam-with-bond model.

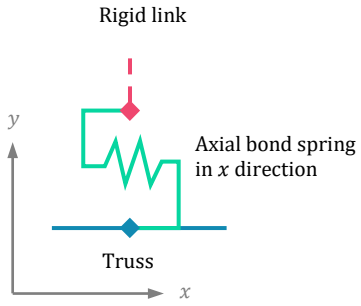

Figure 3: Axial spring configuration in the local initial undeformed configuration.

2.2 Constitutive models

Three different constitutive laws are introduced for concrete, steel and bond-slip interface, respectively.

The concrete model is based on the damage-plastic constitutive law proposed in [21]. This is based on a Bezier interpolation scheme for the damage evolution and a plasticity algorithm, and uses a parameter ranging from 0 to 1 which controls the yielding region, where 0 corresponds to a Drucker-Prager criterion [22] and 1 corresponds to a modified criterion presented in [23]. Another parameter ranging from 0 to 1 controls damage using different interpolation points in tension and compression to allow for a non-symmetric response. The 1D unconfined version is used here. An example of the cyclic behavior is shown in Fig. 4(a).

The steel model is based on Menegotto and Pinto [24], which allows for hardening under a specified b parameter that allows to compute the hardening modulus as a fraction of the Young's modulus. An example is shown in Fig. 4(b).

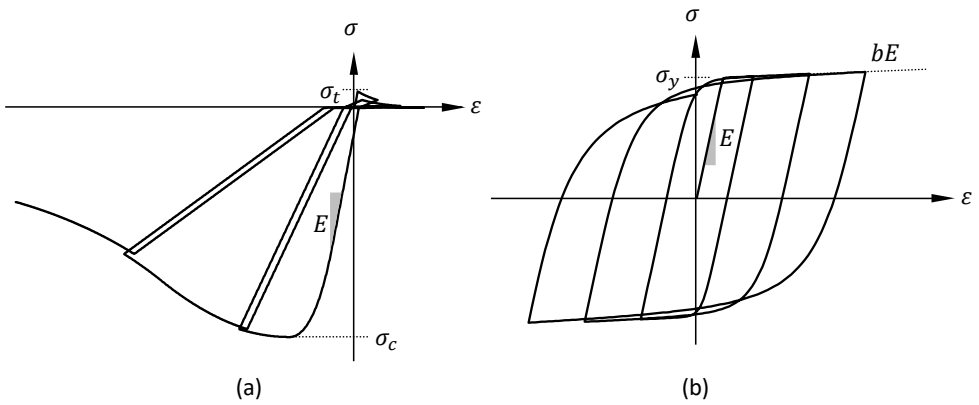

Figure 4: (a) Concrete and (b) steel uniaxial constitutive laws.

The model used for the bond-slip interface is proposed in [25] and implemented in OpenSEES [19]. It is based on a four-points controlled piece-wise linear curve with a return mapping algorithm that emulates a friction-like behavior. An example is shown in Fig. 5.

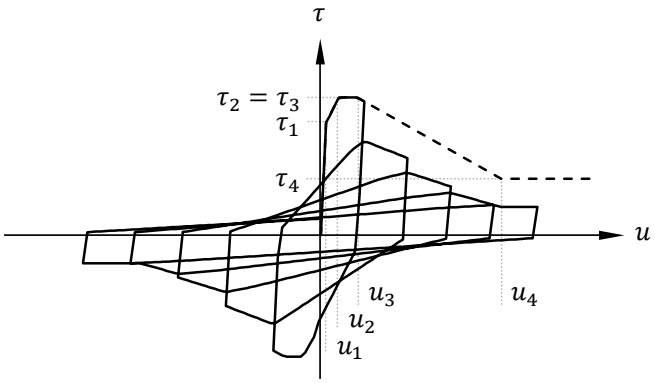

Figure 5: Bond-slip interface constitutive law

2.3 Regularization technique

In attempting to obtain objective results in presence of strain-softening behavior, as in case of reinforced concrete elements, regularization techniques are adopted. This paper investigates the performance of fracture energy-based regularization methods, as these are widely adopted due to their straightforward implementation. In this case, the post-peak softening response is controlled by two different fracture energy parameters, labeled as G_t and G_c for tension and compression, respectively. A characteristic length, l_{ch}, is introduced, evaluated as the ratio of the length of the damaging zone, and the mesh integration length [26]. Other possible local regularization techniques are discussed in [6, 27, 28, 29] An example is shown in Figs. 6a and 6b where, where, if l_{ch} equals one, the constitutive law is the actual experimental response expected for a concrete specimen.

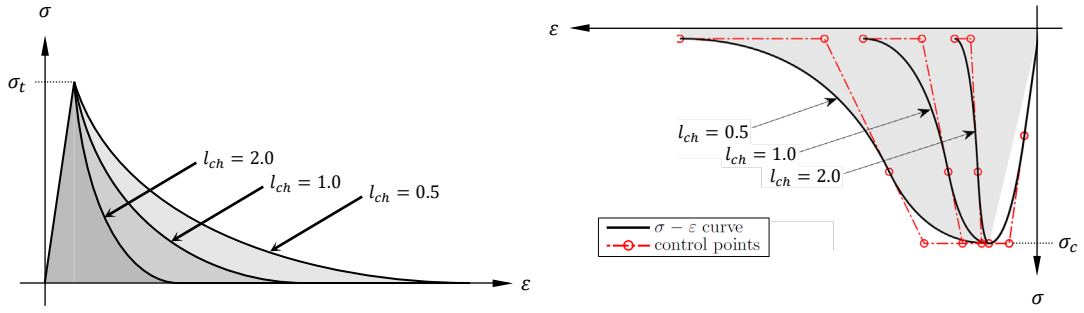

(a) (b)

Figure 6: (a) Tension and (b) compression fracture energy regularization.

3 Results

Since this work focuses on localization at the first cracking, bending tests are performed. Numerical tests on the simple beam schematically shown in Fig. 7 and la-

beled beam J4 in [30] are carried out. Geometric and mechanical data are reported in Table 1. For symmetry, only half of the beam is represented and the left end with restrained rotation is the beam midspan.

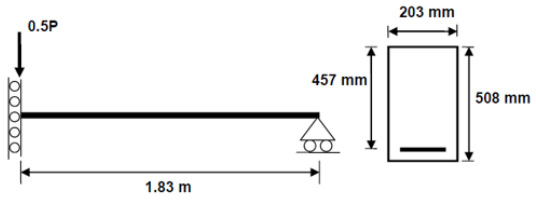

Figure 7: Schematic representation of beam J4.

Concrete		Steel	
$E_c\ [MPa]$	26200	$E_s\ [MPa]$	203395
$f_t\ [MPa]$	2.4	$\sigma_y\ [MPa]$	309.65
$f_c\ [MPa]$	33.24	b	0.01
$G_f\ [N/mm]$	0.0875	$A_s\ [mm^2]$	$100 \div 1000$

Table 1: Geometric and mechanical parameters of beam J4.

3.1 Bending test on plain concrete beam

First, a fiber-section beam model is used to study the numerical response of the unreinforced beam. The beam is discretized using an increasing number of FEs ranging from 10 to 320. In the first test, curvature and axial strain always localize in the first element to the left of midspan, as it is the only one experiencing cracking. In Fig. 8, on the left, the global response is shown for DB and FB elements. A Gauss-Lobatto integration scheme, involving two quadrature points, is used here for both approaches, requiring the FB elements to be regularized considering half mesh length i.e., by using a double fracture energy amount. A similar behavior can here be observed for both approaches, and it is clear that the peak point, that corresponds to the crack formation, keeps moving until eventually, in the limit case labeled as "infty" in Fig. 8(a), concrete does not crack at all and responds as a ductile material. In Fig. 8(b) the fiber tensile response shows the effect of the fracture energy regularization.

Fig. 9 shows the first section top (compression-left) and bottom (tension-right) fibers' strain evolution as the midspan displacement increases. The concrete compression softening branch is never engaged here as concrete cracking leads to sudden element failure and the descending response in compression in Fig. 9 represents stress unloading. Peaks correspond to cracking stages. The two figures clearly show that the fracture energy regularization performs poorly: the post-cracking softening curve is indeed regularized but the overall response is still largely subject to numerical dependencies. Convergence can be achieved when an infinite amount of fracture energy is considered, but this represents a non-realistic case.

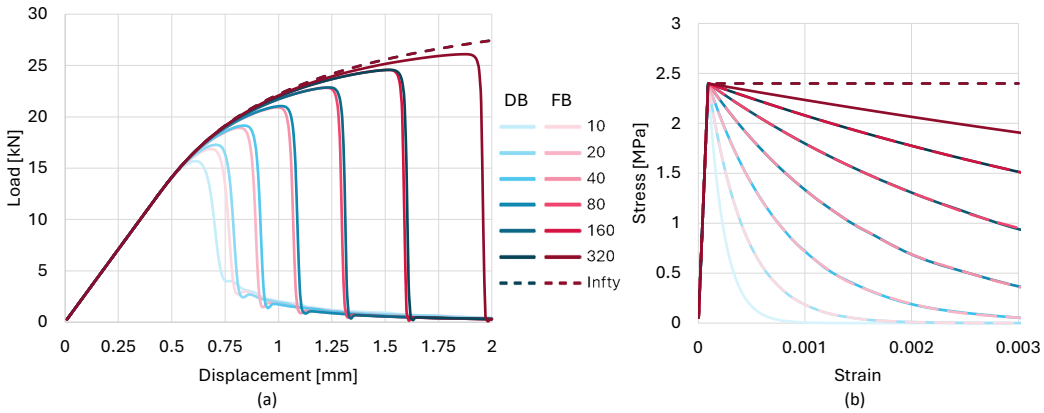

Figure 8: Global response for DB and FB approaches (a) and lower fiber tensile stress vs strain for DB elements (b) for a progressively increasing number of FEs.

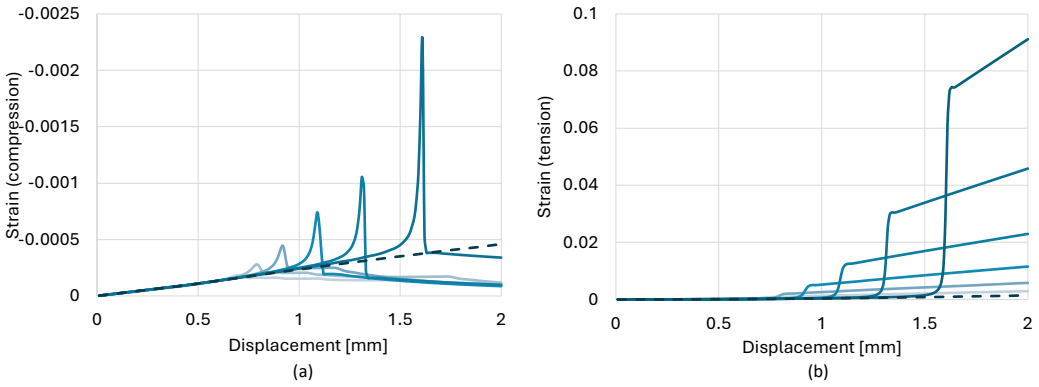

Figure 9: Compressed top fiber strain over global displacement for the DB case (left); tensile fiber strain over global displacement (right).

3.2 Bending tests on reinforced concrete beam with perfect-bond and with bond-slip

This section details the impact of the interaction between concrete and steel under the assumptions of perfect bond and bond-slip. It is organized as follows:

- response of fiber section with perfect-bond beam element;
- response of concrete fiber section beam element plus rebars with bond-slip with different reinforcement ratios and with different bond conditions (perfect-bond and low-bond);
- effect of the mesh refinements with variable reinforcement ratio;
- effect of bond on explicit models;
- non-regularized case for explicit models.

In this section, only results on DB elements are shown since similar outcomes are also expected for FB elements, as shown in Section 3.1 where a plain concrete section is tested. The response of a classical fiber beam with perfect bond is studied first.

A specimen with very little reinforcement ratio ρ is analyzed ($\rho = A_s/A_c = 0.1\%$, where A_s is the steel area and A_c is the concrete section gross area). The mesh is progressively refined, and the response is studied with and without regularization. The aim is to highlight the softening branch after first cracking and display the different behaviors. Fig. 10(a) clearly highlights the effects of the tension fracture energy regularization: the softening branches show similar trends but start at different peak stages. This is clearly shown by the steel response, which yields at different stages for each mesh. Without regularization (Fig. 10(b)), both peaks and softening trends are completely different, as for non-regularized cases, a pathological mesh dependency is expected.

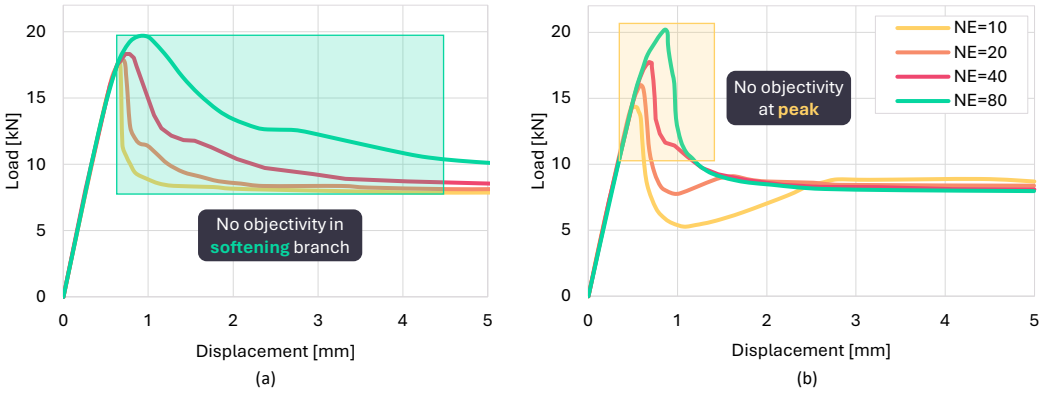

Figure 10: Global responses considering a low amount of steel, equal to $\rho = 0.1\%$, for (a) non-regularized FE model and (b) fracture energy regularized FE model.

The effect of bond is investigated in Fig. 11 for a medium amount of reinforcement $\rho = 0.5\%$. The mesh is discretized with 10 regularized FEs. When the bond is relatively poor, the overall contribution of steel is low and only one crack is formed. When the maximum bond stress is $\tau_{max} > 1$ MPa, more cracks are formed along the beam at an increasing density as the bond intensity improves.

Three different steel reinforcement ratios are used in Fig. 12, $\rho = 0.1\%$, $\rho = 0.5\%$ and $\rho = 1.0\%$. Both perfect-bond and low-bond cases are represented employing explicit modeling: in both cases only one crack at the midspan forms, and the response is overestimated with respect to the experimental case.

By assuming a realistic bond-slip law, as in this case where $\tau_{max} = 2$ MPa, results are non-objective as the mesh changes. Fig. 13 shows that, for three reinforcement ratios and for numbers of FEs from 10 to 1280, the global response does not regularize and convergence is not achieved at the cracking stage.

Fig. 14 shows the evolution of the steel strain for all the considered cases. Although it eventually converges in the hardening stage for highly refined meshes, the yielding strain is different for every case.

Fig. 15 shows the displacement at which the second crack forms (left) and the distance between the first two cracks. The left diagram shows no sign of convergence, and no cracks are observed, in a concentrated sense, for more than 80 FEs. The

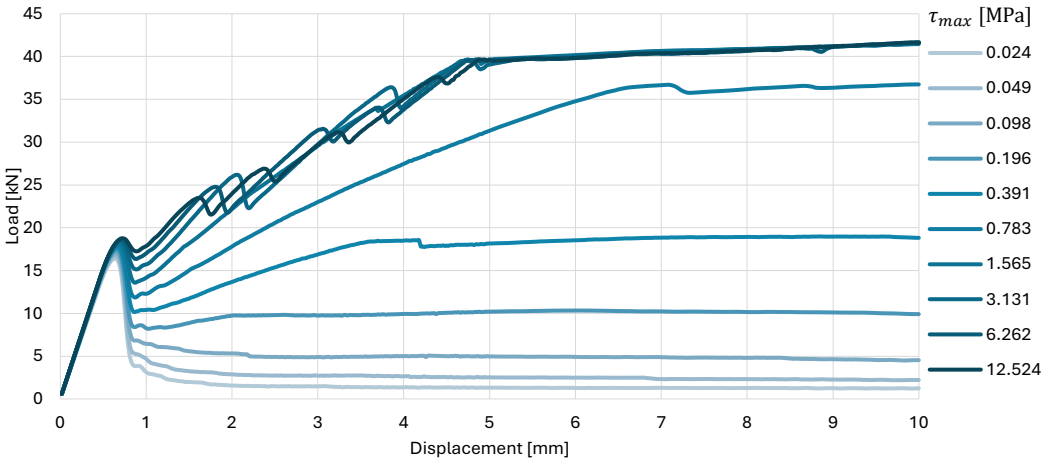

Figure 11: Global response with $\rho = 0.5\%$ with variable bond strength using 10 elements for every case.

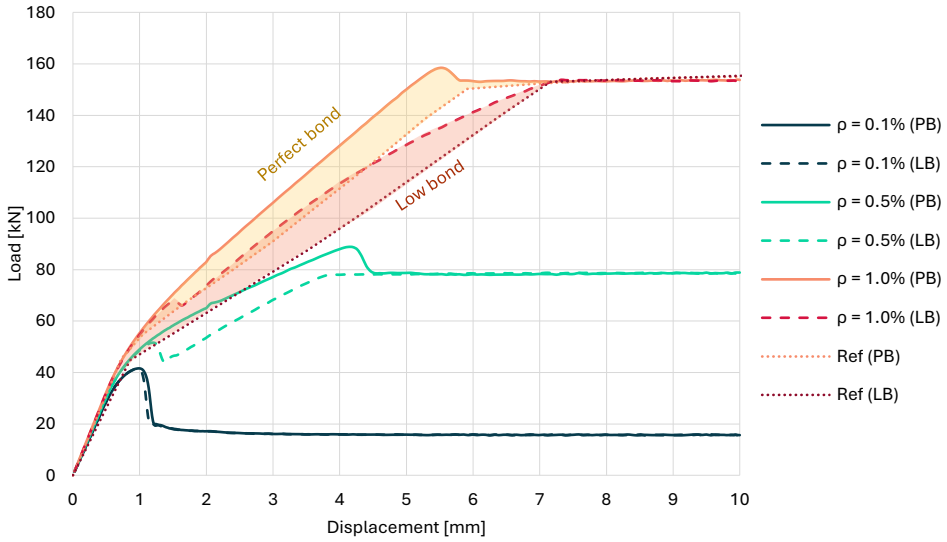

Figure 12: Global response with variable amount of reinforcement ratio ρ using 40 elements to discretize the beam. Experimental comparisons (ref) are reported for perfect- (PB) and low-bond (LB) as a comparison.

right diagram shows that a general correspondence between analytic and numerical results is achieved at 40-80 elements, but there is no overall objectivity. Fig. 16 shows how the steel reinforcement responds in various cases: while the post-yielding steel strain eventually stabilizes for a high number of FEs, the yielding strain occurs at different midspan displacements, which might still differ from the infinite fracture energy limit case. Curvatures and fiber stress for the first three meshes are reported in Fig. 17. Curvature peaks indicate that a crack has opened in that region. Fig. 17(a,b,c) correspond to a lower reinforcement ratio, therefore a lower interaction area and poor bond, while Fig. 17(d,e,f) correspond to a higher reinforcement ratio.

In addition, tests without regularization were intentionally carried out for the $\rho =$

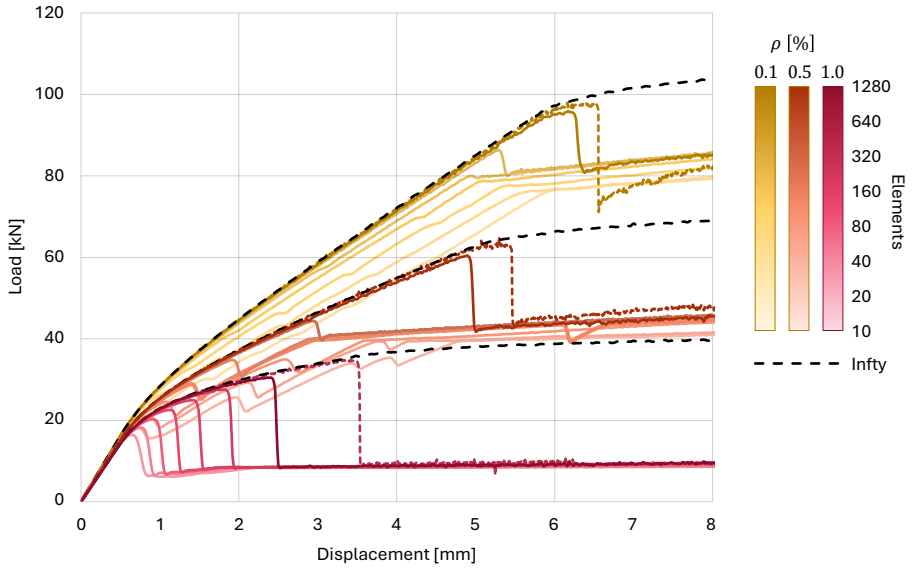

Figure 13: Global response with increasing number of FEs to discretize the beam. Experimental comparisons (ref) are reported for perfect- (PB) and low-bond (LB) as a comparison.

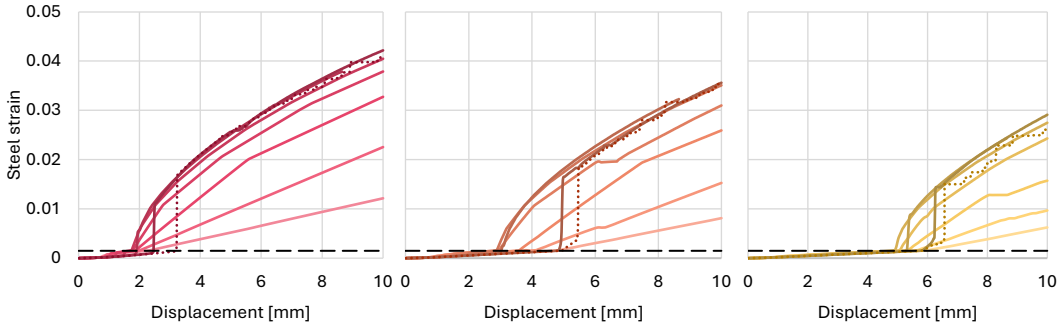

Figure 14: Steel strain vs displacement for all the meshes and $\rho = 0.1 - 0.5 - 1.0\%$ from left to right. The black dashed line represents the steel yielding strain threshold.

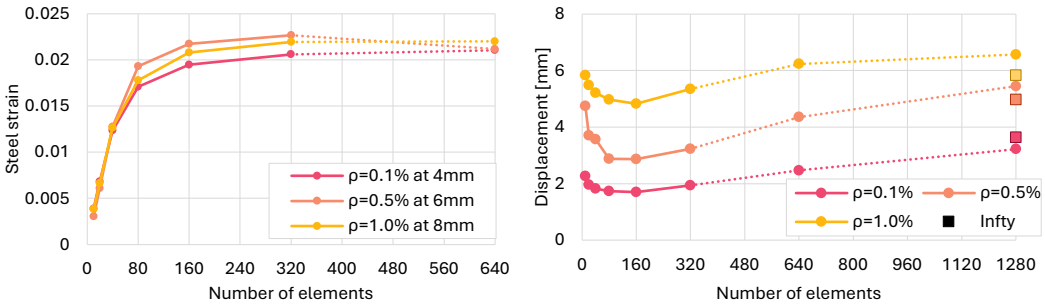

Figure 15: Steel behavior for different reinforcement ratios: (left) steel strain in midspan section at specified displacements and (right) midspan displacement at steel yielding.

0.5% case. As shown in Fig. 18, the resulting curves are quite regular. This regularity arises because, even with the initial mesh, the softening behavior is very stiff due to

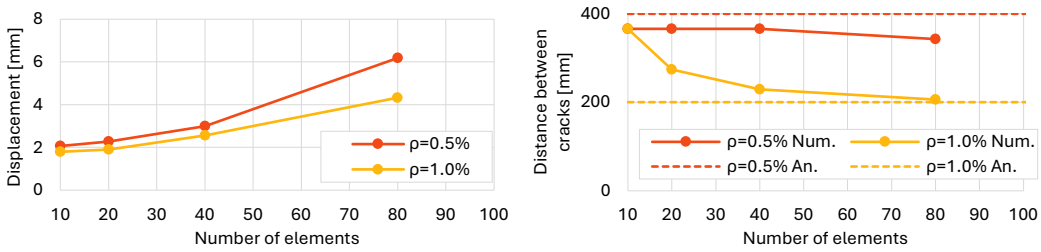

Figure 16: Evolution of cracking for different meshes: (left) midspan displacement corresponding to second crack opening and (right) distance between the first and the second crack.

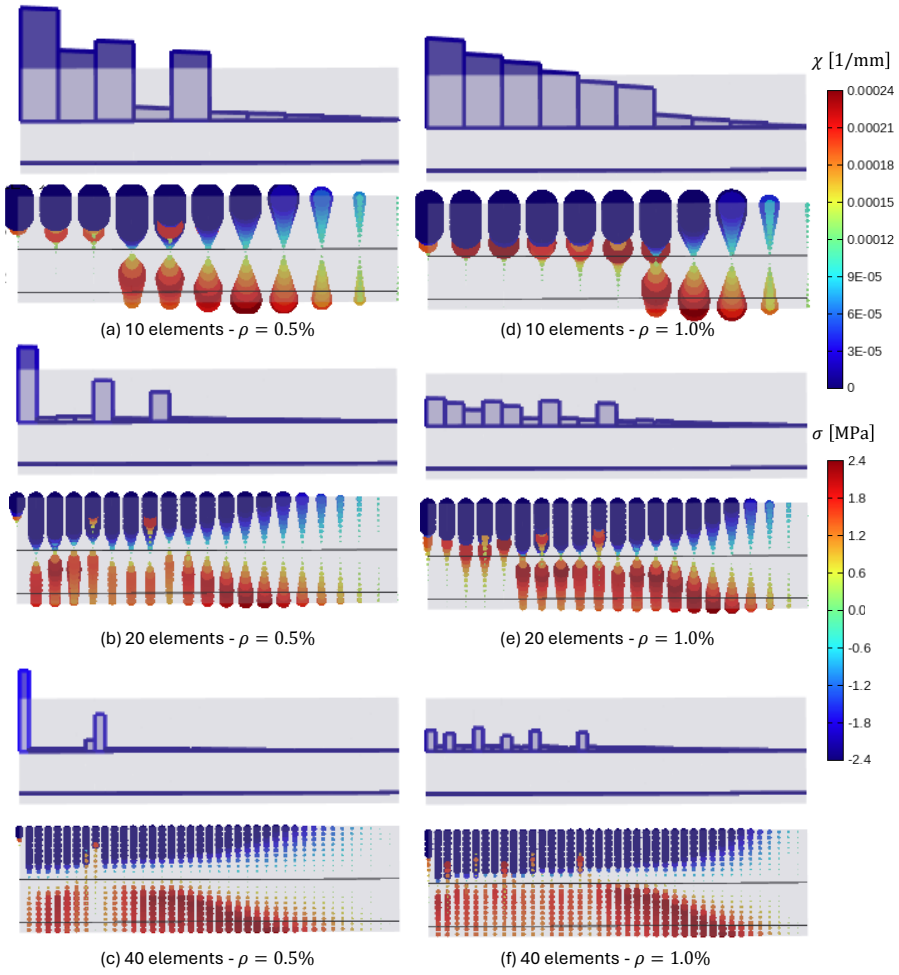

Figure 17: Curvature (top) and fiber stress (bottom) distributions for three meshes and two reinforcement ratios in the pre-yielding stage.

the low tensile fracture energy of concrete. Consequently, there are minimal changes observed as the mesh refines. When examining the curvature distributions, which indicate the cracks' locations, similar patterns emerge across all meshes. This similarity is especially apparent in the finer meshes. However, an unrealistic issue arises: the

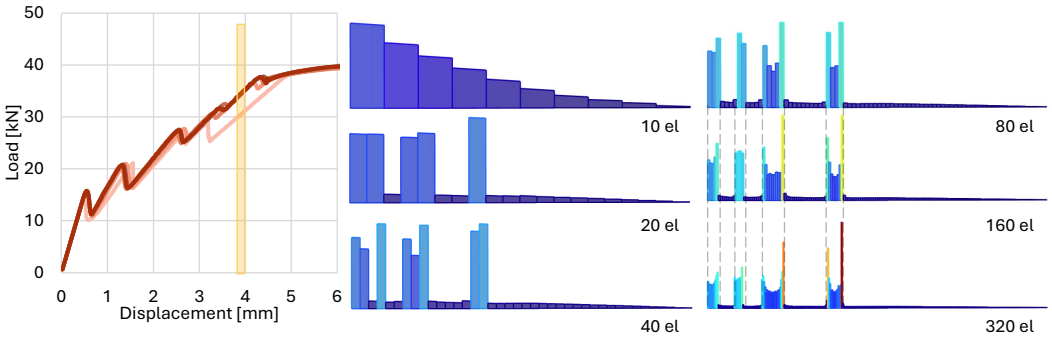

Figure 18: Global structural response for the model without regularization for $\rho = 0.5\%$ (left) and curvatures (right) for different meshes.

curvature tends to spread across adjacent elements. This spread suggests that cracks are diffused, which is not representative of the mechanical behavior of concrete. Thus, this model also fails to accurately capture the expected localized cracking.

4 Concluding remarks

The paper investigates model objectivity and consistency related to strain localization of beam finite element models considering reinforcement that is perfectly bonded or with allowed slip. It is shown that that traditional perfect-bond assumptions can lead to significant inaccuracies, especially in scenarios involving complex loading and crack propagation. Bond-slip models better describe the interactions between concrete and steel reinforcement, although local regularization techniques, such as the fracture energy method, fail to correctly address mesh dependency and realistically capture localized damage. Possible advancements, including higher-order formulations and expanded kinematics as those proposed in [14] are under investigation to obtain more robust and objective structural analyses. Future work should continue to refine these models and explore their applications in diverse structural scenarios, reducing the gap between numerical simulations and real-world behaviors of RC structures.

References

[1] R. De Borst, Some recent developments in computational modelling of concrete fracture, International Journal of Fracture 86 (1997) 5–36.

[2] R. H. J. Peerlings, M. G. D. Geers, R. D. Borst, W. Brekelmans, A critical comparison of nonlocal and gradient-enhanced softening continua, International Journal of solids and Structures 38 (2001) 7723–7746.

[3] E. Åldstedt, P. G. Bergan, Nonlinear Time-Dependent Concrete-Frame Analysis, Journal of the Structural Division 104 (1978) 1077–1092.

[4] C. A. Zeris, S. A. Mahin, Analysis of Reinforced Concrete Beam & Columns under Uniaxial Excitation, Journal of Structural Engineering 114 (1988) 804–820.

[5] E. Spacone, F. C. Filippou, F. F. Taucer, Fibre beam–column element for non-linear analysis of R/C concrete frames: Part I: Formulation, Earthquake Engineering & Structural Dynamics 25 (1996) 711–725.
[6] D. Addessi, V. Ciampi, A regularized force-based beam element with a damage–plastic section constitutive law, International Journal for Numerical Methods in Engineering 70 (2007) 610–629.
[7] D. Addessi, S. Marfia, E. Sacco, A plastic nonlocal damage model, Computer Methods in Applied Mechanics and Engineering 191 (2002) 1291–1310.
[8] M. Petracca, L. Pelà, R. Rossi, S. Oller, G. Camata, E. Spacone, Regularization of first order computational homogenization for multiscale analysis of masonry structures, Computational mechanics 57 (2016) 257–276.
[9] L. Parente, D. Addessi, E. Spacone, A fiber beam element based on plastic and damage models for prestressed concrete structures, Engineering Structures 292 (2023).
[10] P. Di Re, D. Addessi, F. C. Filippou, Mixed 3D Beam Element with Damage Plasticity for the Analysis of RC Members under Warping Torsion, Journal of Structural Engineering 144 (2018) 1–13.
[11] J. M. Hedgepeth, Stress concentrations in filamentary structures, National Aeronautics and Space Administration, 1961.
[12] P. Di Re, D. Addessi, E. Sacco, A multiscale force-based curved beam element for masonry arches, Computers & Structures 208 (2018) 17–31.
[13] D. Addessi, P. Di Re, G. Cimarello, Enriched beam finite element models with torsion and shear warping for the analysis of thin-walled structures, Thin-Walled Structures 159 (2021) 107259.
[14] J. Sio, H. Khalid, B. A. Izzuddin, Objective modelling of reinforced concrete planar frame sub-systems under extreme loading, Structures 60 (2024) 105863.
[15] A. Ayoub, F. C. Filippou, Mixed Formulation of Nonlinear Steel-Concrete Composite Beam Element, Journal of Structural Engineering 126 (2000) 371–381.
[16] A. Ayoub, F. C. Filippou, Finite-Element Model for Pretensioned Prestressed Concrete Girders, Journal of Structural Engineering 136 (2010) 401–409.
[17] C.-L. Lee, F. C. Filippou, Frame Element with Mixed Formulations for Composite and RC Members with Bond Slip. I: Theory and Fixed-End Rotation, Journal of Structural Engineering 141 (2015) 4015039.
[18] S. Limkatanyu, E. Spacone, Reinforced Concrete Frame Element with Bond Interfaces. I: Displacement-Based, Force-Based, and Mixed Formulations, Journal of Structural Engineering 128 (2002) 346–355.
[19] F. McKenna, G. L. Fenves, M. H. Scott, Open System for Earthquake Engineering Simulation, 2000.
[20] M. Petracca, F. Candeloro, G. Camata, Scientific Toolkit for Opensees, 2017.
[21] M. Petracca, L. Pelà, R. Rossi, S. Zaghi, G. Camata, E. Spacone, Micro-scale continuous and discrete numerical models for nonlinear analysis of masonry shear walls, Construction and Building Materials 149 (2017) 296–314.
[22] D. C. Drucker, W. Prager, Soil mechanics and plastic analysis or limit design, Quarterly of Applied Mathematics 10 (1952) 157–165.
[23] J. Lubliner, J. Oliver, S. Oller, E. Oñate, A plastic-damage model for concrete, International Journal of Solids and Structures 25 (1989) 299–326.
[24] M. Menegotto, P. E. Pinto, Slender RC Compressed Members in Biaxial Bending, Journal of the Structural Division 103 (1977) 587–605.

[25] L. N. Lowes, A. Altoontash, Modeling Reinforced-Concrete Beam-Column Joints Subjected to Cyclic Loading, Journal of Structural Engineering-asce 129 (2003) 1686–1697.
[26] M. Petracca, L. Pelà, R. Rossi, S. Oller, G. Camata, E. Spacone, Regularization of first order computational homogenization for multiscale analysis of masonry structures, Computational mechanics 57 (2016) 257–276.
[27] J. Coleman, E. Spacone, Localization issues in force-based frame elements, Journal of Structural Engineering 127 (2001) 1257–1265.
[28] M. H. Scott, G. L. Fenves, Plastic Hinge Integration Methods for Force-Based Beam & Column Elements, Journal of Structural Engineering 132 (2006) 244–252.
[29] M. H. Scott, O. M. Hamutçuoğlu, Numerically consistent regularization of force-based frame elements, International Journal for Numerical Methods in Engineering 76 (2008) 1612–1631.
[30] N. H. Burns, Load-Deformation Characteristics of Beam-Column Connections of Reinforced Concrete, University of Illinois at Urbana-Champaign, 1962.